

I. OLEJARCZYK-WOŹEŃSKA\*, A. ADRIAN\*, H. ADRIAN\*, B. MRZYGLÓD\*

## PARAMETRIC REPRESENTATION OF TTT DIAGRAMS OF ADI CAST IRON

### PARAMETRYCZNA REPREZENTACJA WYKRESÓW CTP<sub>i</sub> ŻELIWA SFEROIDALNEGO

The method of parametric representation of TTT diagrams on example of selected austempered ductile cast irons is presented. TTT diagrams were digitalised and  $n, k$  parameters of Johnson Mehl equation were calculated. The relationships between  $n, k$  parameters and transformation temperature were analysed for two ADI irons. Knowledge of these parameters enables to calculate the progress of austenite to bainite transformation.

*Keywords:* TTT diagrams, austempered ductile iron, bainite transformation

W pracy zaprezentowano metodykę parametrycznej reprezentacji wykresów CTP<sub>i</sub> na przykładzie wybranych wykresów dla żeliw sferoidalnych. Wykresy CTP<sub>i</sub> digitalizowano, a następnie obliczano parametry  $n$  i  $k$  równania Johnsona-Mehla opisującego postęp przemiany przechłodzonego austenitu w bainit. Analizowano wpływ temperatury przemiany na wartość parametrów  $n, k$ . Znajomość tych parametrów pozwala obliczać postęp przemiany austenitu w bainit przy danej temperaturze.

### 1. Introduction

Cast iron is one of the most popular cast alloy used to produce mechanical devices. The interest in the wide use of cast iron arises from simplicity of manufacturing technology, low costs and casting of components to near final shape. However, the modern industry requires to develop new casting materials whose mechanical and physical properties satisfy the designer's requirements [1-3].

One of the cast structure material fulfilling these properties is austempered ductile iron (ADI). ADI is cast iron with excellent combination of strength, plasticity and toughness. Because of those special properties, ADI has been used for a wide variety of applications in automotive, rail, agricultural industry and heavy engineering industry. ADI meets to those unique properties due to its microstructure, which is obtained by an isothermal heat-treatment process. This cast iron has a metallic matrix consisting of ferrite needles and stable austenite saturated with carbon [4-6].

The heat treatment is composed of five stages (Fig. 1): 1 – heating to austenitizing temperature,  $T_\gamma$  (line 1-2), 2 – soaking cast in austenitizing temperature during the time ( $t_\gamma$ ) which assures temperature equalization on cross-section of the casting, decomposition of initial components of cast iron and saturation with carbon (2-3),

3 – cast cooling to an isothermal soaking temperature ( $T_{pi}$ ) at a rate prevents the formation of pearlite (3-4), 4 – isothermal soaking by time ( $t_{pi}$ ) assuring formation of ausferrite structure (4-5), 5 – cooling of the cast to ambient temperature (5-6) [4, 8].

Final structure and properties of ADI are strongly dependent on parameters of an isothermal heat-treatment process. These parameters depend mainly on the chemical composition, geometry, size of microsegregation, content and shape of graphite in the cast iron. The limit values of these parameters are:

- austenitization temperature ( $T_\gamma$ ) 820-950°C,
- austenitization time ( $t_\gamma$ ) 0,5-3h,
- isothermal transformation temperature ( $T_{pi}$ ) 230-400°C,
- time of isothermal transformation ( $t_{pi}$ ) 0,5-5h [3, 4].

At higher temperatures of isothermal soaking ( $T_{pi} = 350 \div 400^\circ\text{C}$ ) upper bainite (upper ausferrite) is formed which contains about 40% austenite  $\gamma$  and about 60% ferrite  $\alpha$ . At lower temperatures, within 250 - 300°C lower bainite (lower ausferrite) is formed containing about 10% austenite  $\gamma$  and 90% ferrite  $\alpha$ . Reduction of the quenching temperature causes the increase of the yield point ( $R_m$ ) and hardness but decreases elongation and impact strength.

\* FACULTY OF METALS ENGINEERING AND INDUSTRIAL COMPUTER SCIENCE AGH UNIVERSITY OF SCIENCE AND TECHNOLOGY, 30-059 KRAKÓW, 30 MICKIEWICZA AV., POLAND

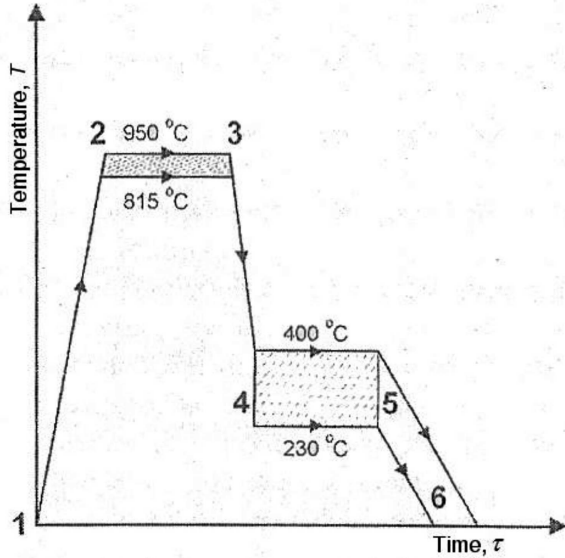


Fig. 1. Schematic illustration of all stages of austempering heat treatment [7]

For the purpose of obtaining suitable properties of ADI cast iron the TTT diagrams are useful. The diagrams allow to set the value of the parameters of the heat treatment process allowing to obtain the expected properties of cast iron.

**2. Experimental material and methods**

A TTT diagram is a plot of temperature versus the logarithm of time for steel or cast iron of definite composition. The TTT diagram illustrates the required time for transformation of austenite to various phases at a constant temperature. It is used to determine when transformations begin and end for an isothermal heat treatment of a previously austenitized material [9].

These charts are crucial in an isothermal heat-treatment process of cast iron with a ferritic-austenitic matrix structure. Based on these diagrams process parameters being determined. TTT diagrams for cast iron with defined composition allow control of the isothermal transformation process and obtain various austenite contents in the matrix (5-40%). However, graphs for ductile iron are scarcely found in descriptive literature [9].

**2.1. TTT diagrams for selected ductile irons**

Two TTT diagrams for austempered ductile iron with different chemical compositions were used. The chemical composition of the first material (to be termed ductile iron 1): 3.2% C, 2.4% Si, 0.21% Mn, 0.59% Ni, 0.62% Cu i 0.13% Mo [10]. Second austempered ductile iron (to be termed ductile iron 2) contains: 3,6%C,

0,27% Mn i 1,72% Si [11]. The TTT diagram for ductile iron 1 were prepared in a range of temperature from 500°C to 250°C. The second chart was drawn in a range from 850°C to 250°C. TTT diagrams for investigated austempered ductile irons are presented in the Fig. 2.

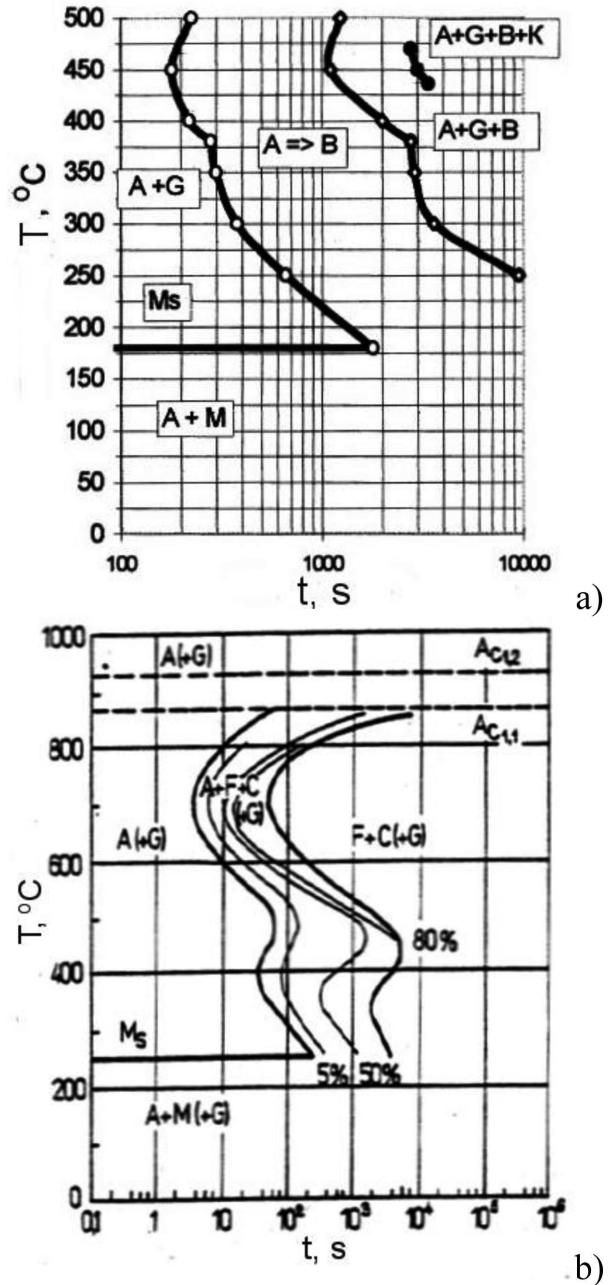


Fig. 2. TTT diagram for austempered ductile iron, a) ductile iron 1, b) ductile iron 2 [10, 11]

Fig. 2a demonstrates that the bainitic transformation (ductile iron 1) occurs in two temperature ranges. The first interval (500-390°C) illustrates the formation of upper bainite, the second (390-250°C) that of lower bainite. Additionally two minimal incubation times, at 450°C in the upper temperature range and at 360°C in the lower temperature interval, can be registered [10].

For the ductile iron 2 the temperature range of bainitic transformation is 500-250°C.

## 2.2. Digitization of TTT diagrams

Sigma ScanPro4 was used to digitalize graphs presented in Fig. 2. It is used e.g. for image analysis, measuring the length of the segment and the size of angles, as well as measuring the distance between two points and the distance on the set path. Thereafter the range of variables were fixed on the axes of ordinates and abscissa. In the next step digitalized points were marked on the TTT curves and coordinate values were assigned to these points. The result of digitalization was a tabular form of analyzed relationships. Obtained values were transferred to Excel and then used to draw TTT curves (Fig. 3, 4). In these figures the existed phases are described as: G – graphite, B – bainite and K – carbides.

## 2.3. Mathematical description of TTT diagrams

The Johnson-Mehl kinetic equation was used to mathematically describe of TTT diagrams:

$$y = 1 - \exp(-kt^n) \quad (1)$$

where:  $y$  – fraction of transformed austenite,  $t$  – time,  $k$ ,  $n$  – parameters related to the temperature.

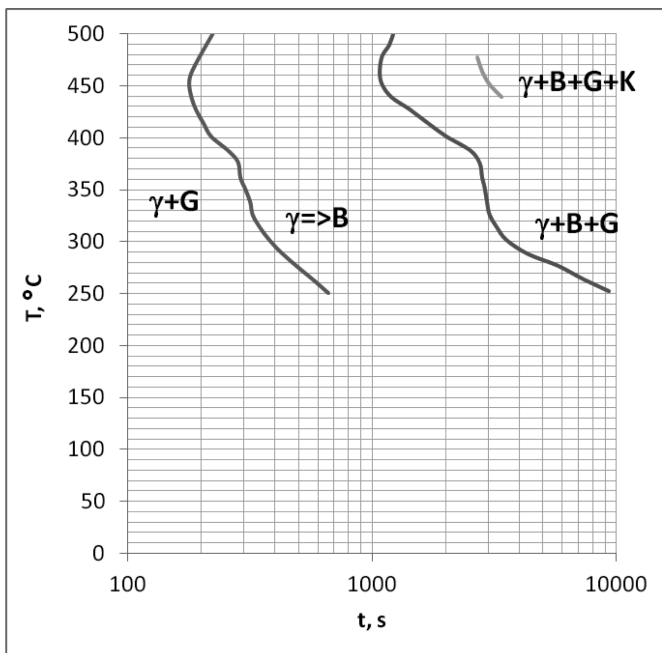


Fig. 3. TTT diagram for the ductile iron 1 after digitalization

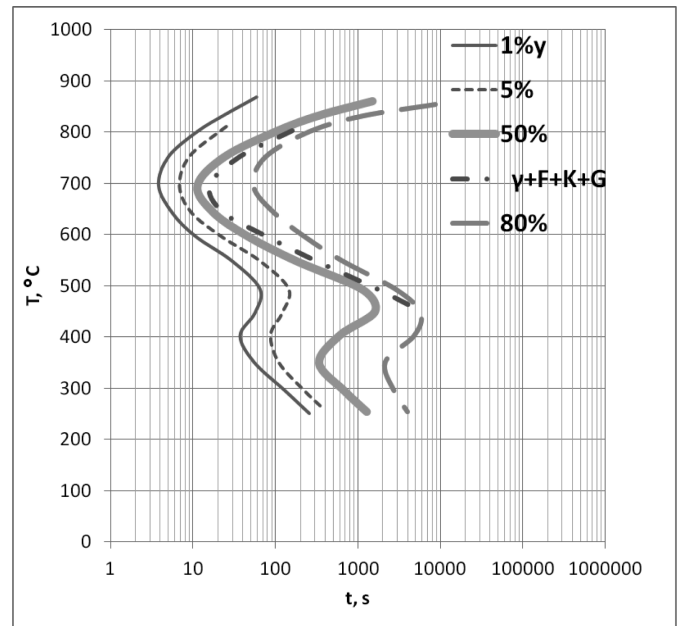


Fig. 4. TTT diagram for the ductile iron 2 after digitalization

The parameters  $k$  and  $n$  are determined due to points coordinates for the beginning ( $t_p, y_p$ ) and end ( $t_k, y_k$ ) of transformation at a certain temperature. In order to determine the parameters  $k$  and  $n$  the equation 1 should be transformed as follows:

$$\ln(k) + n \ln(t_i) = \ln\left(\ln\left(\frac{1}{1 - y_i}\right)\right) \quad (2)$$

where:  $t_i$  – period of time after which the fraction of transformed austenite is  $y_i$ . Knowledge of  $n$  and  $k$  parameters enables to calculate the progress of austenite transformation at relevant temperature.

For steel, for the beginning of the transformation (at a given temperature) usually time  $t_p$  is taken at which the fraction of transformed austenite is  $y_p = 1\%$ , for the end – time  $t_k$  at which  $y_k = 99\%$ . However, the transformation of austenite presented in the analyzed graphs is incomplete. The first curve on TTT diagram for the ductile iron 1 (Fig. 2a) shows the criterion  $y_p = 1\%$ , the second curve was drawn for a different content of bainite. Fig. 5 shows the relationship between volume fraction of austenite and temperature after isothermal soaking. It is in the range of 250-400°C.

As mentioned earlier the volume fraction of transformed austenite in bainite for ductile iron 1 changes with temperature, whereby the value of volume fraction,  $y_k$ , is determined from the relation:  $V_{\text{bainite}} = f(T)$  (Fig. 5). It was used to calculate the parameters  $k$  and  $n$ .

For the ductile iron 2 parameters  $k$  and  $n$  were calculated assuming that 80% of austenite ( $y_k = 80\%$ ) was transformed to bainite.

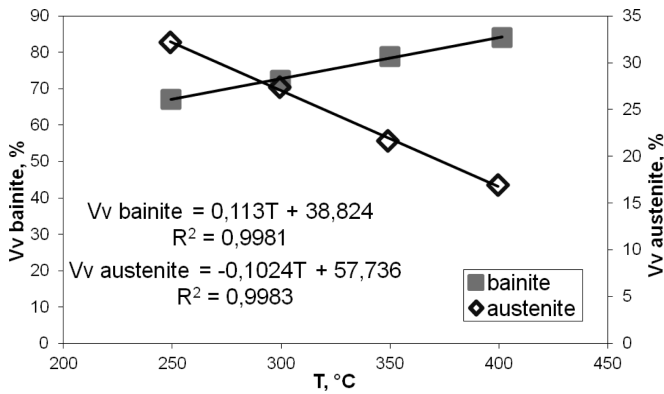


Fig. 5. The volume fraction of the retained austenite and of the bainite vs. the transformation temperature [10]

The relationships between parameters  $k$ ,  $n$  and isothermal soaking temperature for both ductile irons are presented in Fig. 6.

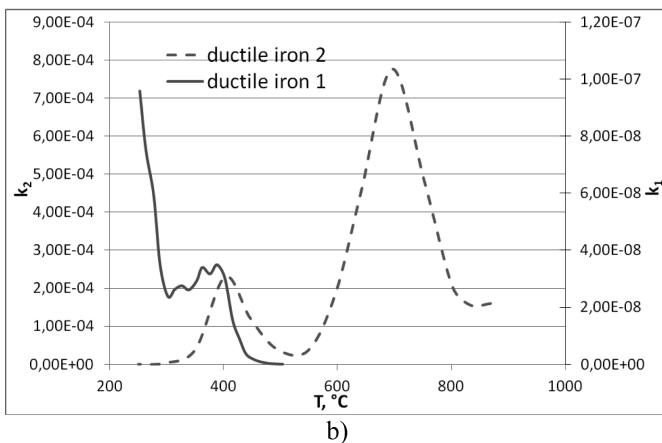
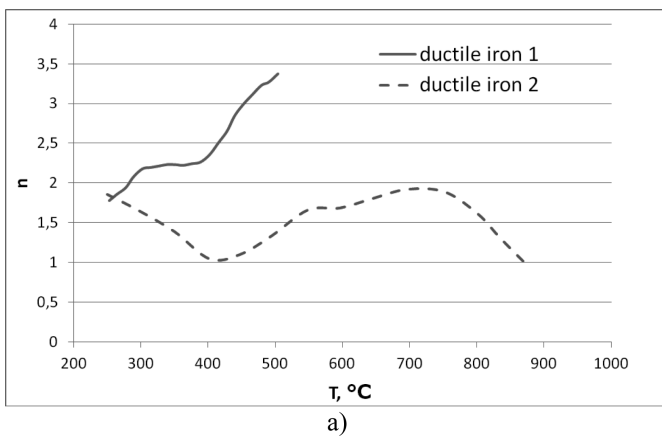


Fig. 6. Relationship between parameters  $k$ ,  $n$  and isothermal soaking temperature, a)  $n = f(T)$ , b)  $k = f(T)$

### 3. Concluding remarks

TTT diagrams are crucial in the heat treatment process. They allow to choose the process parameters so that the desired microstructure and corresponding mechanical properties are obtained. Two TTT diagrams for

different ductile irons were analyzed. For the mathematical description of TTT diagrams for selected austempered ductile iron the Johnson-Mehl equation was applied and parameters  $n$ ,  $k$  were calculated. The values of parameters  $n$  for analyzed ductile irons are in the range  $1.78 \div 3.37$  (ductile iron 1) and  $1.02 \div 1.92$  (ductile iron 2), those  $k$  are:  $3.56 \cdot 10^{-11} \div 3.34 \cdot 10^{-9}$  (ductile iron 1) and  $3.45 \cdot 10^{-7} \div 7.78 \cdot 10^{-4}$  (ductile iron 2). Different trends in changes of parameters  $n$  and  $k$  with the temperature changes for selected ductile irons, can be observed.

Ductile iron 1, containing more alloying elements, causes parameters  $n$  to increase with rising temperature in the range of bainitic transformation. The parameter  $k$  decreases in the temperature range  $250 \div 300^\circ\text{C}$ , then increases in  $300 \div 400^\circ\text{C}$  and decreases again after reaching  $400^\circ\text{C}$ .

For ductile iron 2 the value of  $n$  (in the temperature range of bainite transformation) decreases with rising temperature to  $400^\circ\text{C}$  and then begins to increase. Parameter  $k$  behaves differently: its value increases in the temperature range  $250 \div 400^\circ\text{C}$ , then starts decreasing to a temperature of approximately  $500^\circ\text{C}$ . A similar changes of  $k$  can be observed in the temperature range of a pearlite transformation.

In summary the differences in the values of  $n$  and  $k$  parameters for both analyzed ADI irons were observed. They may be caused by different chemical compositions of the analyzed cast irons. The alloying elements (Ni, Cu, Mn) contained in the ductile iron 1 highly decrease the value of  $k$  compared to ductile iron 2.

### Acknowledgements

The financial support from the Ministry of Science and Higher Education, contract No N N508 585539 is gratefully acknowledged.

### REFERENCES

- [1] A. Rimmer, Kosten- und Leistungsvorteile Getriebekomponenten aus ADI. Giesserei-Erfahrungsaust, 5, 32-33 (2008).
- [2] J.R. Laub, D. Durkee, Converting to ADI with Concurrent Engineering, Eng.Cast.Solutions 8, 6, 30-32 (2006).
- [3] R. Biernacki, J. Kozłowski, D. Myszk, P. Perzyk, Prediction of Properties of Austempered Ductile Iron Assisted by Artificial Neural Network, Materials Science (Medžiagotyra) 12, 1, (2006).
- [4] A. Białobrzęski, J. Pezda, Testing of heating and cooling process of ADI cast iron with use of ATND method, AFE 8, 11-14 (2008).
- [5] A. Vasko, The factors influencing microstructure and mechanical properties of ADI, AFE 9, 133-136 (2009).

- [6] M.C. Cakir, A. Bayram, Y. Isik, B. Salar, The effects of austempering temperature and time onto the mechainability of austempered ductile iron, *Mater. Sci. Eng. A* **407**, 147-153 (2005).
- [7] D. Myszk a, M. Kaczorowski, B. Tybulczyk, Źeliwo sferoidalne ausferrytyczne bezpośrednio hartowane izotermicznie, Wyd. Instytut Odlewnictwa, Kraków 2003.
- [8] Forum Inżynierskie. Rozwój technologii Źeliwa ADI w Polsce. Wyd. Instytut Odlewnictwa, Kraków 2009.
- [9] J. Pacyna [edited by], *Metaloznawstwo wybrane zagadnienia*, WND AGH, Kraków 2005.
- [10] A. Kutsov, Y. Taran, K. Uzlov, A. Krimmel, M. Evsyukov, Formation of bainite in ductile iron, *Mater. Sci. Eng. A* **273-275**, 480-484 (1999).
- [11] A. Özcan, M.Sc. thesis, The Middle East Technical University, Ankara 2003.
- [12] SigmaScan Pro Automated Image Analysis Software, User's manual, Jandel Scientific Software 1995.

*Received: 10 November 2011.*